HYGROTHERMAL BEHAVIOR AT THE JUNCTION OF CEMENT MORTAR AND BIOBASED MATERIALS
Finite Element Study of Hempcrete, Date Palm Concrete, and Clay Brick

by

Mourad BENDEKHIS[a], Naima FEZZIOUI[b], Mebirika BENYAMINE[c], Noureddine KAID[d], Samia LARGUECH[e], Mustafa BAYRAM[f*], Younes MENNI[d,g], and Salih OZER[h]

[a] Laboratory of Energetic in Arid Zones (ENERGARID), Mechanical Engineering Department, Faculty of Technology, Tahri Mohamed University, Bechar, Algeria
[b] Laboratory of Mechanics of Structures L. M. S., Civil Engineering and Hydraulics Department, Faculty of Technology, Tahri Mohamed University, Bechar, Algeria
[c] Laboratory of Reliability of Materials and Structures in the South-FIMAS, Mechanical Engineering Department, Faculty of Technology, Tahri Mohamed University, Bechar, Algeria
[d] Department of Mechanical Engineering, Institute of Technology, University Center Salhi Ahmed Naama (Ctr. Univ. Naama), Naama, Algeria
[e] Department of Electrical Engineering, College of Engineering, Princess Nourah bint Abdulrahman University, Riyadh, Saudi Arabia
[f] Department of Computer Engineering, Biruni University, Istanbul, Turkey
[g] College of Technical Engineering, National University of Science and Technology, Dhi Qar, Iraq
[h] Mus Alparslan University, Mechanical Engineering, Mus, Turkiye

Original scientific paper
https://doi.org/10.2298/TSCI2504239B

This study investigates the hygrothermal behavior at the junction between cement mortar and three biobased materials, hempcrete, date palm concrete, and clay brick, using the finite element method. Numerical simulations were conducted under both summer and winter conditions to analyze temperature and relative humidity distributions across a multilayer block at a depth of 145 mm. The results reveal that each material exhibits a distinct hygrothermal signature. Hempcrete ensures stable moisture buffering and smooth gradient transitions. Date palm concrete offers high moisture transfer and insulation performance, but with sharper discontinuities. Clay brick shows intermediate behavior with moderate buffering and more gradual junction transitions. The finite element method results highlight the junction as a critical zone where mismatches in material properties can lead to moisture accumulation, mechanical stresses, and durability concerns. These findings underscore the importance of selecting compatible materials and designing junctions carefully to ensure long-term performance and comfort in biobased building envelopes.

Key words: *biobased materials, junction, moisture transfer, heat transfer, seasonal boundary conditions*

Introduction

In the pursuit of sustainable construction practices, biobased concretes have emerged as promising alternatives to conventional building materials due to their favorable environmen-

* Corresponding author, e-mail: mustafabayram@biruni.edu.tr

tal profile and multifunctional properties. Recent research has focused on understanding the complex interplay between the physical, mechanical, and hygrothermal characteristics of these materials. Paiva *et al*. [1] investigated the role of bioaggregates in influencing the hygrothermal behavior of bioconcretes, establishing foundational knowledge on the impact of natural inclusions. Extending this line of inquiry, Belloum *et al*. [2] assessed the hygrothermal performance of buildings constructed with date palm-based concrete, reinforcing the practical applicability of such materials in real-world environments. Several studies have explored the integration of PCM into bioconcretes to enhance thermal regulation. Wu *et al*. [3, 4] examined biobased concretes incorporating PCM, showcasing significant improvements in thermal buffering and energy performance. Similarly, Benkhaled *et al*. [5] conducted a sensitivity analysis on hygrothermal models for hemp concrete, enhancing the predictive capacity for material behavior under variable conditions. Ferroukhi *et al*. [6] and Affan *et al*. [7] highlighted the importance of material composition and microencapsulation techniques in optimizing both hygrothermal and mechanical performance.

Understanding moisture hysteresis and its implications on thermal transfer has become a pivotal area of study. Benmahiddine *et al*. [8] conducted multi-scale analyses to evaluate these effects in hemp concrete. Ayati *et al*. [9] and Aguiar *et al*. [10] expanded the material scope to include hybrid composites and fire performance evaluations of wood-based bioconcretes. Further approaches were undertaken by Wu *et al*. [11], who developed multilayer biobased envelopes to improve energy efficiency. The material selection and fiber reinforcement strategy remain critical. Charai *et al.* [12] explored the use of Alfa fibers, while Bennai *et al*. [13] compared hemp concrete to traditional materials at building scale. El Moussi *et al*. [14] examined rice straw's influence on straw-lime concretes, providing a pathway for utilizing agricultural waste. Earlier foundational work by Chennouf *et al*. [15] established date palm fiber concrete as a viable thermal insulating alternative.

Comprehensive reviews such as that by Ansari *et al*. [16] have synthesized knowledge on hemp-based concretes, highlighting the low carbon potential of such systems. Ahmad and Chen [17] delved into the effects of aggregate size and binder types, offering insights for tailoring material performance. Sawadogo *et al*. [18] presented novel biobased PCM-hemp concretes aimed at passive energy storage, reinforcing the multifunctionality of these systems.

Ntimugura *et al*. [19] introduced Miscrete, an innovative lime-miscanthus blend, as a low carbon insulation material, broadening the palette of available biocomposites. Alioua *et al*. [20] contributed through a sensitivity study on date palm concrete, addressing transient heat and moisture transport. Pietrak *et al*. [21] offered comparative permeability analyses between magnesium-hemp and lime-hemp concretes, underscoring measurement challenges in hygrothermal studies. The durability and environmental interaction of bioconcretes have also been addressed. Benmahiddine *et al*. [22] studied the impact of immersion and drying cycles, while Lagouin *et al*. [23] explored how binder and aggregate types influence performance. Advanced modelling of hysteresis in heat and mass transfer has been developed by Zou *et al*. [24], contributing to the theoretical framework needed for accurate simulation. Finally, the work by Benmahiddine *et al*. [25] on flax concrete emphasized how variations in aggregate size and content affect key material properties.

This study aims to investigate the hygrothermal behavior at the junction between cement mortar (CM) and three biobased construction materials, hempcrete, date palm concrete (DPC), and clay brick, using the FEM. The objective is to characterize heat and moisture transfer across these material interfaces under realistic summer and winter boundary conditions. By analyzing temperature and relative humidity distributions at a critical wall depth, the study

seeks to identify discontinuities, buffering capacities, and potential risks related to material incompatibility.

Modelling heat and moisture transfer

This study investigates the hygrothermal behavior of a multilayer composite concrete block composed of a conventional mortar-cement layer and a biosourced concrete sub-block. The composite element, illustrated in fig. 1, consists of an upper mortar-cement concrete block measuring 290 × 195 × 445 mm^3, cast over a biosourced concrete block of 140 × 90 × 290 mm^3. The internal surface exposed to indoor boundary conditions is divided between the biosourced material (90 × 290 mm^2) and the mortar-cement section (195 × 445 mm^2), while the entire external surface (195 × 445 mm^2) is formed by the mortar-cement material and subjected to ambient conditions. The geometry and internal composition of the block are further detailed in fig. 2 through cross-sectional views (C-C, A-A, B-B) and directional lines.

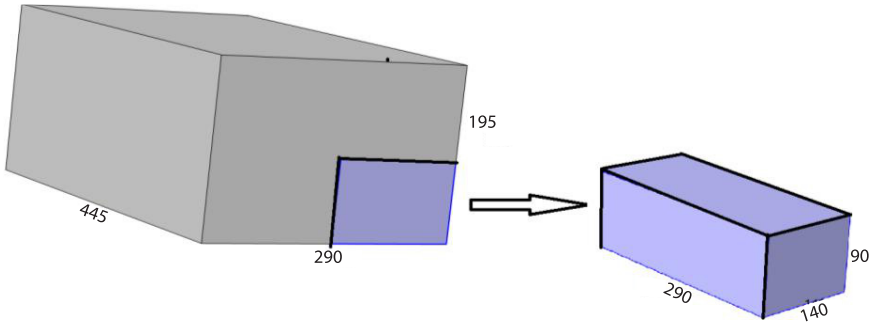

Figure 1. Composite block of mortar-cement and biosourced concrete

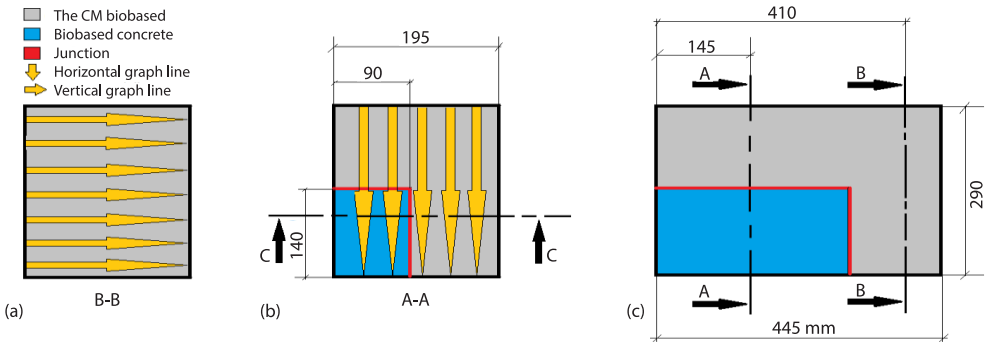

Figure 2. Cross-sections (A-A, B-B, C-C) of the multilayer composite block showing CM and biosourced concrete

To model the physical behavior of this system, the study focuses on the coupled heat and mass transfer phenomena occurring in porous materials, under a set of simplifying assumptions. Each material is treated as a homogeneous and isotropic medium. Moisture transfer mechanisms are considered according to the level of relative humidity: starting with vapor-only diffusion at low humidity, followed by condensation and evaporation due to the formation of liquid bridges, then parallel vapor-liquid transport including surface diffusion, and finally liquid-flow in saturated conditions. Hysteresis effects are not included in the current model. The behavior is based solely on adsorption and absorption data, without accounting for desorption. Additionally, the interface between the mortar-cement and biosourced concrete layers is assumed to be in perfect contact, ensuring continuous heat and moisture flow across the boundary.

The heat transfer model includes conduction through the solid matrix (Fourier's Law) and latent heat effects due to vapor diffusion. The governing equation is [26]:

$$\rho c \frac{\partial T}{\partial t} = \nabla\left(\lambda \nabla T\right) + L_{\mathrm{v}} \nabla\left(\frac{\delta_a}{\mu} \nabla\left(\phi p_{\mathrm{v,sat}}\right)\right) \tag{1}$$

The moisture transport is driven by gradients in relative humidity and vapor pressure. The governing equation, expressed using relative humidity as the driving potential [26]:

$$\frac{\partial w}{\partial \phi} \frac{\partial \phi}{\partial t} = \nabla\left(D_{\mathrm{w}} \frac{\partial w}{\partial \phi} \nabla \phi\right) + \nabla\left[\frac{\delta_{\mathrm{a}}}{\mu} \nabla\left(\phi p_{\mathrm{v,sat}}\right)\right] \tag{2}$$

where ρ is the bulk density, c – the specific heat capacity, and T – the temperature. The parameter λ is the thermal conductivity and L_{v} – the latent heat of vaporization of water. The term δ_{a} [kgm^{-1}s^{-1}Pa^{-1}] represents the vapor permeability in air and μ – the vapor diffusion resistance factor. The ϕ is the relative humidity, $p_{\mathrm{v,sat}}$ [Pa] – the saturation vapor pressure at T, w – the moisture content, and D_{w} – the liquid water diffusivity.

The hygrothermal behavior of the multilayer block is modeled as a porous medium, where heat and moisture transport are governed by coupled differential equations. This thermo-hydric coupling captures the strong interaction between temperature and moisture, reflecting their mutual influence on material performance.

Material properties that are strongly temperature-dependent include the water vapor permeability of still air, δ_{a}, the saturation vapor pressure, $p_{\mathrm{v,sat}}$, and the capillary absorption coefficient, A_{w}. These parameters are essential for accurately describing vapor diffusion and latent heat effects within the porous structure. Detailed formulations for these parameters can be found in [27-31]. In addition temperature-dependent properties, several material properties are analytically defined as functions of relative humidity, ϕ. These include thermal conductivity, $\lambda(w)$, moisture content, $w(\phi)$, liquid water diffusivity, $D_{\mathrm{w}}(\phi)$, and volumetric heat capacity, ρc (ϕ). These relationships are critical for simulating realistic heat and moisture transfer in heterogeneous and hygroscopic materials. The specific analytical expressions for these parameters used in this study are based on data from [32-35]. For detailed information on the material properties used in this study, refer to Alioua *et al.* [36] for DPC, Seng [37] for hemp concrete (HAMP), Ramirez *et al.* [38] and D'Altri *et al.* [39] for CM, and both Ghiassi *et al.* [40] and Ramirez *et al.* [38] for clay brick. These studies provide the hygro-thermal parameters essential for accurate modelling and simulation of each material's behavior under coupled heat and moisture conditions.

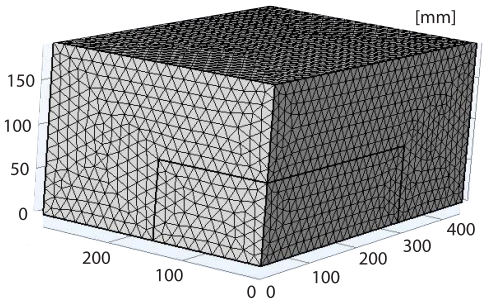

Figure 3. Finite element mesh of the multilayer block

The hygrothermal simulations used boundary conditions for winter and summer, along with uniform initial conditions. A Neumann approach was applied, specifying heat and moisture fluxes through convective transfer. The initial temperature and relative humidity were set at 20 °C and 50%, respectively. Internally, both seasons used T_{in} = 20 °C and ϕ_{in} = 45%. Externally, winter conditions were T_{ext} = 13 °C, ϕ_{ext} = 65%, and summer conditions were T_{ext} = 40 °C and ϕ_{ext} = 12%. Heat transfer coefficients were $h_{T,\mathrm{ext}}$ = 25 W/m^{2}K, and $h_{T,\mathrm{in}}$ = 8 W/m^{2}K, while moisture transfer coefficients were $h_{\mathrm{m,ext}}$ = $2.0 \cdot 10^{-7}$ Wm^{2}K, and $h_{T,\mathrm{in}}$ = $3.0 \cdot 10^{-8}$ W/m^{2}K [41].

The finite element mesh used for the simulation of the multilayer block is shown in fig. 3. It consists of a 3-D unstructured grid primarily composed of tetrahedral elements. The geometry was discretized into 110168 tetrahedra and 6432 triangular surface elements, with a total of 19756 mesh vertices. According to the mesh statistics, the average element quality (based on skewness) is 0.6623, while the minimum element quality is 0.2011, reflecting acceptable mesh performance for numerical accuracy. The element volume ratio is 0.0765, and the total mesh volume is approximately $2.516 \cdot 10^7$ mm^3. The FEM was used to solve the governing equations of coupled heat and moisture transfer within the multilayer structure.

For validation, the numerical results are compared with those reported by Ramirez *et al*. [26], under similar boundary and material conditions. The temperature evolution across the wythe brick masonry wall, comprising bricks and CM joints along section A-A′ (top), is analyzed using a time-dependent (transient) simulation. For further details on this validation, see Fezzioui *et al*. [42]. The comparison shows good agreement between the numerical predictions and the reference data [26], confirming the accuracy and reliability of the implemented hygrothermal model.

Results and discussion

To assess junction behavior, a reference depth of 145 mm, intersecting the CM/biobased interface, was selected at the midpoint of the biobased material. Simulations for winter and summer were conducted, with results extracted along horizontal lines to evaluate seasonal thermo-hydric performance. The location of the selected depth and the corresponding graph lines for data extraction are illustrated in fig. 2 (cross-section A-A). Figure 4 presents the temperature distribution along the multilayer block at a depth of 145 mm under summer conditions for three material pairings: CM combined with DPC, Hemp concrete, and Clay Brick. The results provide insight into the thermal resistance and interface effects of each configuration. Figure 4(a) illustrates that hempcrete, when exposed to a temperature of 40 °C, conducts heat inward with a linearly decreasing temperature gradient, a result of its high thermal resistance. At the interface between the CM and hempcrete, a negative thermal bridge is observed, where the markedly lower thermal conductivity of hempcrete serves as a thermal barrier. This pronounced thermal contrast brings about important hygrothermal implications. First, the cold zone represented by the hempcrete may promote condensation under winter conditions. Additionally, the hygroscopic nature of hempcrete, with a water absorption capacity of 429 kg/m^3, enhances the coupling between thermal and moisture behavior. Furthermore, the disparity in vapor permeability between the two materials can lead to localized moisture accumulation. From a system energy performance perspective, this configuration reveals an asymmetric thermal behavior: hempcrete functions as an efficient thermal insulator on the interior side, while the CM contributes thermal inertia and external protection. The sharp thermal gradient observed within the hempcrete zone demonstrates its capacity to limit heat loss, thereby contributing to the optimized energy performance of the composite wall system. As illustrated in fig. 4(b), the CM shows minimal temperature change (40-34.2 °C) over the initial region, indicating quasi-isothermal behavior due to its moderate conductivity and thermal inertia. A clear inflection point at the CM/DPC interface marks a sharp shift in thermal behavior. The DPC layer that follows exhibits a steady linear gradient from 34.2 °C down to 20 °C, highlighting its high thermal resistance and effective insulation. The thermal discontinuity at the junction confirms the presence of a thermal barrier, while the regular gradient beyond it suggests smooth heat diffusion and reduced thermal bridging. Figure 4(c) reveals a rapid temperature decrease from 40-32.7 °C in the CM, pointing to its relatively high conductivity.

After the CM/brick interface, the clay brick layer demonstrates a more gradual temperature drop to 20 °C, showing better insulation and higher thermal resistance. The inflection at 32.7 °C indicates a thermal mismatch at the junction, with heat accumulating in the mortar and delayed transfer into the brick. Beyond the interface, the profile stabilizes, showing the material's ability to regulate heat flow over distance.

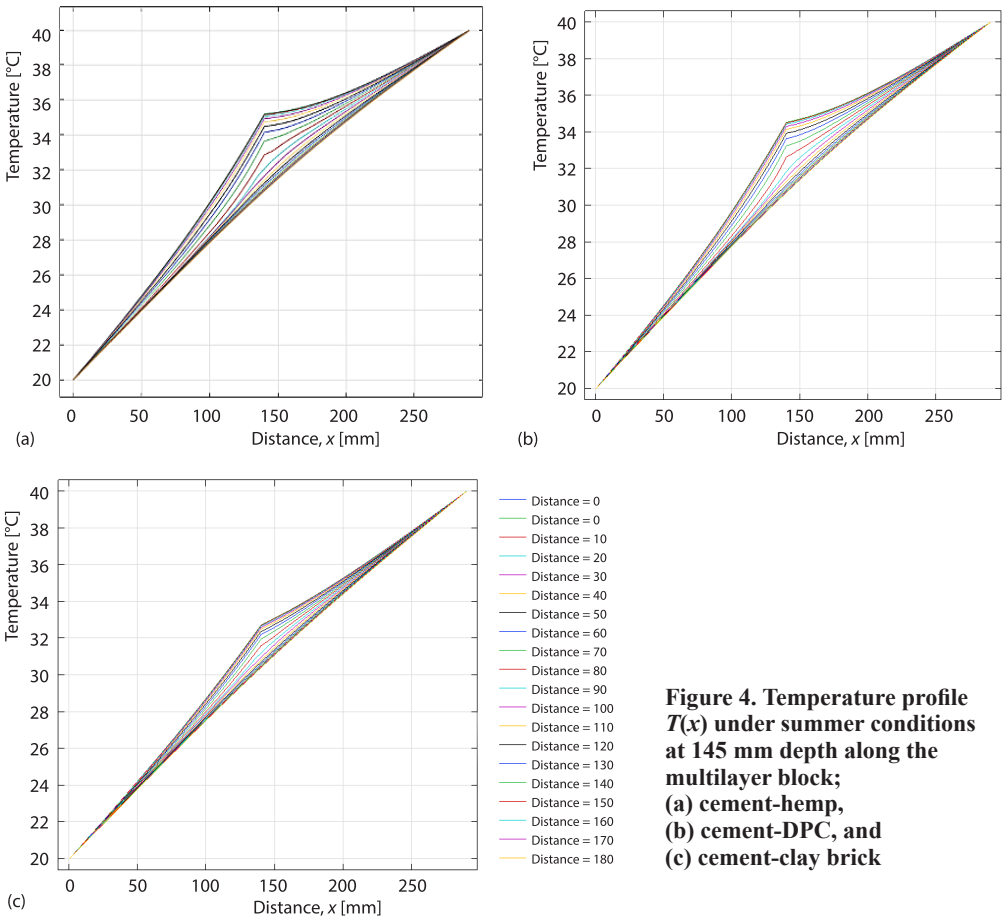

Figure 4. Temperature profile $T(x)$ under summer conditions at 145 mm depth along the multilayer block; (a) cement-hemp, (b) cement-DPC, and (c) cement-clay brick

Figure 5(a) illustrates the wintertime temperature distribution measured at a depth of 145 mm within multilayer blocks composed of three different junctions: CM-hempcrete, CM-DPC, and CM-clay brick. The simulations are conducted under typical winter conditions, with the interior temperature maintained at 20 °C and the exterior boundary exposed to 13 °C, allowing for a detailed analysis of heat propagation across each composite interface. At the CM/hempcrete interface, heat accumulation occurs, slowing the rate of heat dissipation. The high outdoor humidity (65%) promotes partial condensation at the interface, releasing latent heat and locally increasing the temperature. As a result, the composite block exhibits heterogeneous thermal behavior, marked by a distinct discontinuity at the interface. While hempcrete provides effective thermal insulation, the interface with the CM emerges as a critical zone that requires careful consideration optimize overall system performance. Accounting for hygrothermal coupling is essential to accurately predict real-world behavior under operational conditions. This analysis highlights the complex yet intriguing thermal characteristics of the com-

posite block. The discontinuity observed at x = 140 mm directly reflects the significant contrast in thermophysical properties between the two materials. Although each material demonstrates quasi-linear thermal behavior in accordance with Fourier's Law, their junction forms a critical transition zone that warrants special attention in the system's design and optimization. In the CM-DPC configuration, as reported in fig. 5(b), the temperature in the CM rises slightly from 13-14.9 °C, showing a minimal gradient due to its moderate thermal resistance and possible latent heat release.

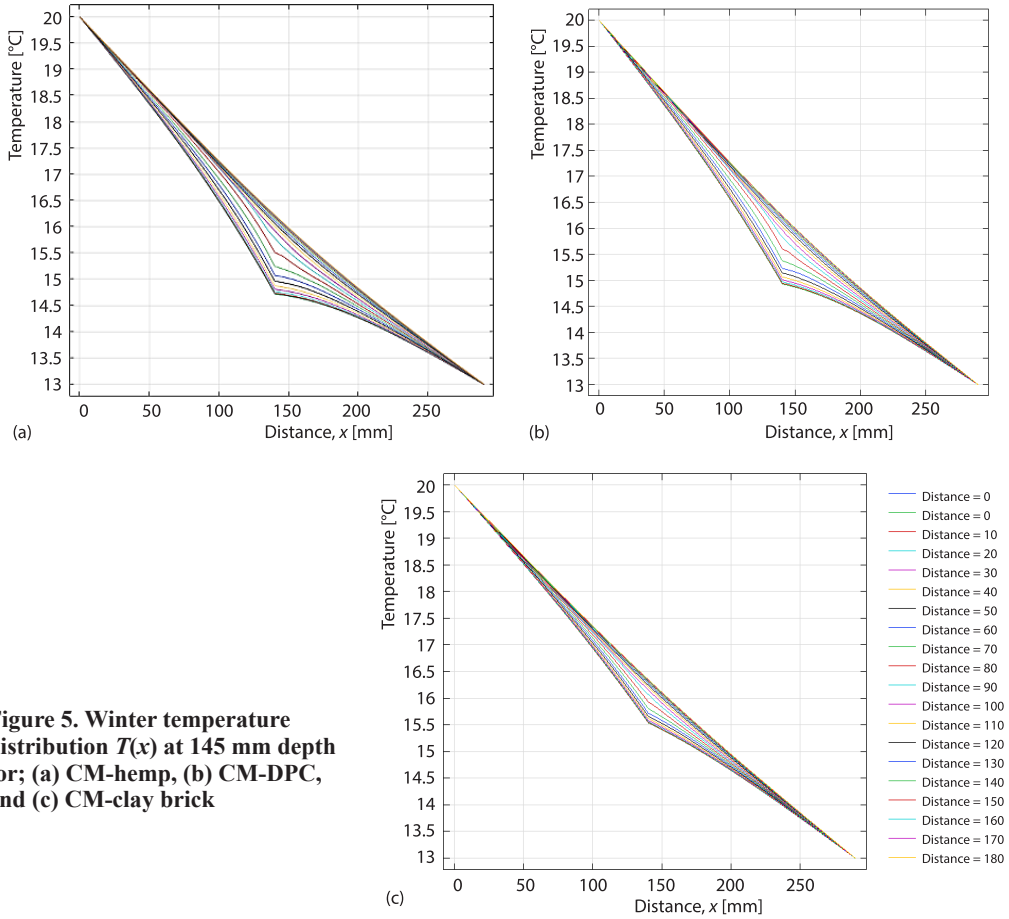

Figure 5. Winter temperature distribution $T(x)$ at 145 mm depth for; (a) CM-hemp, (b) CM-DPC, and (c) CM-clay brick

At the interface, a sharp inflection at 14.9 °C reveals a strong thermal barrier between the materials. The DPC layer then displays a quasi-linear temperature increase from 14.9 °C to 20 °C, confirming its high thermal resistance and strong insulating performance. The temperature profile stabilizes further from the junction, showing that the influence of the interface decreases with depth, and DPC maintains its effectiveness in limiting heat loss. In the CM-clay brick configuration, as illustrated in fig. 5(c), the CM shows a rapid temperature rise from 13-15.4 °C across four lines, reflecting high thermal conductivity and low resistance. After the junction, the clay brick layer sees a smoother increase to 20 °C, indicating better thermal insulation and higher resistance. The transition at 15.4 °C highlights the interface as a thermal discontinuity, with a barrier effect that slows heat transfer. Though the clay brick provides

effective insulation beyond the interface, the junction zone remains sensitive and can impact overall performance, particularly under dynamic weather conditions.

Figures 6 and 7 depict the relative humidity profiles at a fixed depth of 145 mm under summer and winter conditions, with curves corresponding to various horizontal positions. The relative humidity distribution reveals three distinct zones:

– Zones 1. Non-linear region in the CM before the junction.
– Zones 2. Quasi-linear transition through the biobased concrete.
– Zones 3. Gradual relative humidity variation in the CM beyond the joint.

The inflection point between Zones 1 and 2 highlights a clear discontinuity in hygric behavior across the interface.

The analysis of moisture behavior within the CM-hempcrete composite block reveals complex transport phenomena driven by the contrasting hygroscopic properties of the constituent materials and the influence of boundary conditions. The results demonstrates a distinctly asymmetric moisture distribution, with significant variations observed across different zones, fig. 6(a).

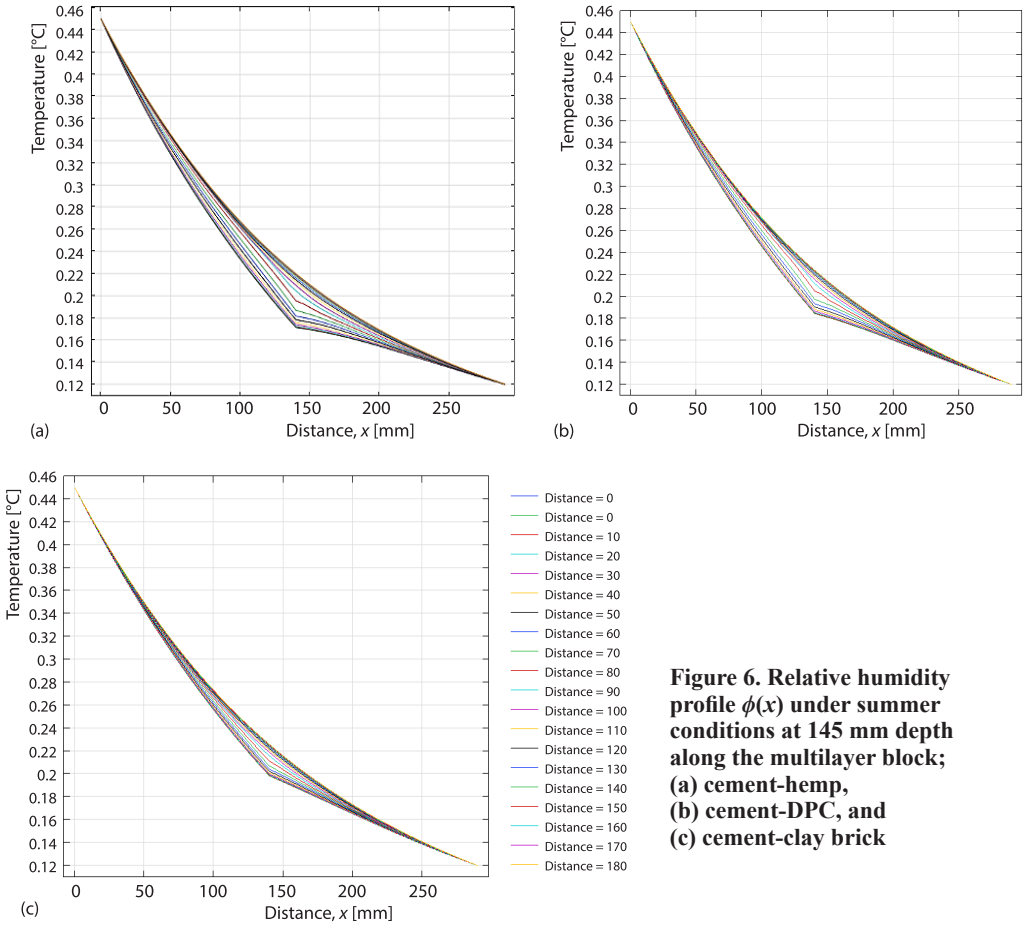

Figure 6. Relative humidity profile $\phi(x)$ under summer conditions at 145 mm depth along the multilayer block; (a) cement-hemp, (b) cement-DPC, and (c) cement-clay brick

Zone 1 (0-140 mm), corresponding to the CM (graph line: 0-80 mm): relative humidity decreases from $\phi = 0.45$ to $\phi = 0.17$, highlighting the low hygroscopic capacity of the CM. This gradual decline is attributed to its relatively high vapor resistance factor

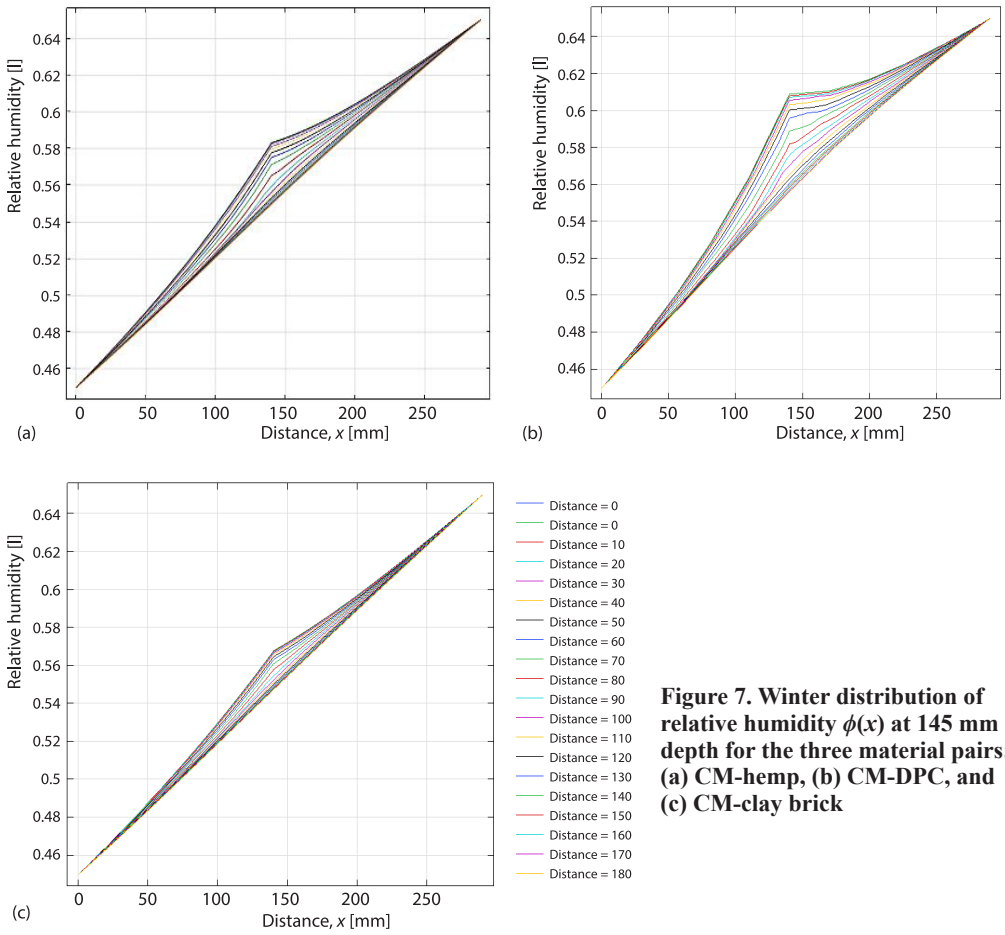

Figure 7. Winter distribution of relative humidity $\phi(x)$ at 145 mm depth for the three material pairs; (a) CM-hemp, (b) CM-DPC, and (c) CM-clay brick

(μ = 25) and low capillary water content (w_{cap} = 180 kg/m³). The quasi-exponential profile reflects vapor diffusion through a low porosity, low permeability medium. Zone 2 (140-290 mm), corresponding to hempcrete (graph line: 0-80 mm): At the interface (x = 140 mm), a pronounced transition in moisture behavior occurs. Hempcrete, with its significantly lower vapor resistance (μ = 6.31) and high capillary water uptake (w_{cap} = 429 kg/m³), exhibits a smoother relative humidity gradient, typical of a hygroscopic material capable of buffering moisture. The inflection point at x = 140 mm marks a major moisture discontinuity, resulting from:

– A strong contrast in vapor permeability ($\delta_p \approx 3.16 \cdot 10^{-11}$ kg/msPa *vs*. much lower for CM),
– Substantial differences in adsorption/desorption characteristics,
– Disparities in water absorption coefficients (A = 0.165 vs. 0.06 kg/m²s$^{0.5}$).

This discontinuity may lead to localized moisture accumulation at the interface, which is particularly critical under winter conditions. Zone 3 (0-290 mm), representing a second CM segment (graph line: 80-180 mm): this region captures the evolution of relative humidity within the mortar extending beyond the horizontal junction, showing a gradient from ϕ = 0.12 (external side) to ϕ = 0.45 (internal side). This range represents the steepest humidity gradient in the entire composite. It results directly from the imposed boundary conditions: summer external conditions (T_{ext} = 40 °C, ϕ_{ext} = 12%) and interior conditions (T_{int} = 20 °C, ϕ_{int} = 45%). The pro-

file in this zone exhibits a curvature characteristic of diffusion in a semi-infinite medium, with an exponentially decreasing shape that reflects the dominant influence of the external environment on this part of the CM.

In the CM/DPC configuration, fig. 6(b), relative humidity increases from 12%-18.4% in Zone 1 with a near-linear gradient, followed by a steeper rise up to 45% in Zone 2 after the junction. The DPC's high absorption and permeability accelerate moisture uptake, creating a distinct humidity step and underlining its excellent moisture buffering in summer. Finally, for the CM/clay brick system, fig. 6(c), relative humidity evolves similarly, with a rise from 12%-19.8% in CM, followed by a sharp, non-linear increase in the brick layer up to 45%. The inflection point again highlights the interface transition. Across all three systems, relative humidity gradients are steeper after the junction, demonstrating the superior hygric responsiveness of the biobased materials. Notably, vertical divergence in relative humidity curves increases closer to the interface, suggesting the influence of multidirectional vapor diffusion.

Figures 7(a)-7(c) illustrate the winter relative humidity profiles across three composite block, CM combined with Hempcrete, DPC, and Clay Brick, highlighting distinct moisture behaviors under winter boundary conditions (T_{ext} = 13 °C, ϕ_{ext} = 65%; T_{int} = 20 °C, ϕ_{int} = 45%). In fig. 7(a), analysis of this graph reveals a fundamentally different relative humidity behavior than that observed in summer conditions, which has major consequences for the performance of the composite system.

Zone 1 – Hempcrete (0-140 mm):

This zone exhibits progressive moisture accumulation, with relative humidity increasing from 0.45-0.61 (ΔRH = +0.16), while maintaining a quasi-linear trend. Hempcrete, characterized by high hygroscopicity (A = 0.165 kg/m^{2}s$^{0.5}$), w_{cap} = 429 kg/m^3), actively absorbs and stores moisture originating from the humid exterior environment. Its low vapor resistance (μ = 6.31) facilitates the uptake of external humidity (ϕ_{ext} = 65%), allowing hempcrete to function as an effective hygric buffer during winter conditions.

Zone 2 – Interface and CM (140-290 mm):

At the interface (x = 140 mm), relative humidity peaks at 0.61 and continues to rise to 0.65 within the CM. This area becomes a critical point of moisture convergence. Despite the cement mortar's low vapor permeability (μ = 25), it exhibits unexpected moisture accumulation. The rise in relative humidity from 0.61-0.65 suggests the formation of a stagnation zone, where moisture transfer is hindered due to the material's inherent resistance. This behavior is particularly concerning, as it indicates moisture retention in a material not designed for storage, potentially leading to long-term degradation or reduced thermal performance.

Figure 7(b) presents the CM-DPC system, where relative humidity decreases non-linearly from 65%-61% before the junction, then sharply to 45% within the DPC, reflecting its efficient vapor transport due to superior permeability and absorption coefficients. Beyond the junction, the relative humidity gradient stabilizes, illustrating a steady diffusion regime. In fig. 7(c), the CM-Clay Brick profile shows a quasi-linear relative humidity decrease from 65%-56% in the CM region, followed by a non-linear drop to 45% within the clay brick layer, driven by the brick's favorable hygroscopic properties and high capillarity. The interface again marks a distinct change in slope due to contrasting material properties like vapor resistance (μ = 25 for CM *vs*. 34.14 for clay brick) and thermal conductivity. Together, these plots in fig. 7 emphasize how material selection and interface characteristics critically influence moisture distribution during winter, with biobased components generally promoting better regulation, while the CM tends to trap moisture near junctions.

The junction between CM and biobased concretes presents critical hygrothermal behaviors with significant implications for building durability and indoor comfort. Results highlight a marked discontinuity at the interface (x = 140 mm), resulting from contrasting properties such as vapor resistance (μ = 25 for CM *vs*. 34.14 for clay brick), thermal conductivity (1.72 *vs*. 0.59 W/mK), and water absorption coefficients (0.06 *vs*. 0.104 kg/m^{2}s$^{0.5}$).

These disparities create a physical barrier to continuous moisture flow, causing water stress concentrations and potential internal condensation in winter. Such abrupt changes in water content can generate mechanical stresses due to differential expansion/contraction cycles, ultimately leading to debonding, cracking, or interface degradation over time. However, biobased materials such as DPC demonstrate superior hygric behavior. Their high saturated water content (429 kg/m³ for DPC vs. 180 kg/m³ for cement mortar) and strong vapor permeability enable efficient moisture buffering and rapid redistribution in response to boundary conditions.

As shown in relative humidity profiles, particularly in Zone 1, complex moisture fluxes develop due to both material heterogeneity and horizontal distance variations, indicating multidirectional diffusion that reinforces the dynamic role of the interface. In summer, with internal humidity higher than the exterior (ϕ_{int} = 45%, ϕ_{ext} = 12%), materials like clay brick show higher moisture retention on the interior side, offering thermal and hygric inertia beneficial for indoor comfort without artificial humidification. Though less efficient than hempcrete or DPC in buffering, clay brick provides a more gradual moisture transition across the junction, reducing abrupt hygric shocks and promoting durability. The interface thus acts not merely as a passive boundary but as an active hygrothermal mediator, requiring careful material pairing to mitigate stress concentrations and optimize building envelope performance under varying seasonal conditions.

Conclusion

The numerical simulations carried out using FEM enabled a detailed analysis of the hygrothermal behavior of junctions between cement mortar and three biobased materials, hempcrete, DPC, and clay brick, under both summer and winter conditions. The results showed that disparities in vapor resistance, thermal conductivity, and moisture absorption lead to pronounced discontinuities at the junction, especially in winter. Hempcrete displayed stable and gradual moisture transitions, making it suitable for buffering humidity. The DPC exhibited superior moisture transfer and insulation but introduced sharper hygrothermal discontinuities. Clay brick demonstrated balanced, intermediate performance. Overall, the junction acts as a sensitive zone influencing both comfort and durability. Thus, proper material pairing and interface design are essential to optimize the performance of multilayer biobased wall systems.

Acknowledgment

Princess Nourah bint Abdulrahman University Researchers Supporting Project number (PNURSP2025R826), Princess Nourah bint Abdulrahman University, Riyadh, Saudi Arabia.

References

[1] Paiva, R. D. L. M., *et al*., Influence of Bioaggregates on the Physical and Hygrothermal Properties of Bioconcretes, *Construction and Building Materials*, *456* (2024), 139218
[2] Belloum, R., *et al*., Hygrothermal Performance Assessment of a Biobased Building Made with Date Palm Concrete Walls, *Building and Environmen*t, *223* (2022), 109467
[3] Wu, D., *et al*., Simulation of the Hygrothermal Behavior of a Building Envelope Based on Phase Change Materials and a Biobased Concrete, *Fluid Dynamics and Materials Processing*, *18* (2022), 5, pp. 1483-1494

[4] Wu, D., *et al*., Multilayer Assembly of Phase Change Material and Biobased Concrete: A Passive Envelope to Improve the Energy and Hygrothermal Performance of Buildings, *Energy Conversion and Management*, *257* (2022), 115454
[5] Benkhaled, M., *et al.*, Sensitivity Analysis of the Parameters for Assessing a Hygrothermal Transfer Model Ham in Biobased Hemp Concrete Material, *International Communications in Heat and Mass Transfer*, *132* (2022), 105884
[6] Ferroukhi, M. Y., *et al*., Impact of Microencapsulated Phase Change Material on a Biobased Building Composite, *Hygrothermal and Mechanical Behavior*, *Construction and Building Materials*, *409* (2023), 133925
[7] Affan, H., *et al*., Comparative Analysis of Biobased Insulation Materials with Low-Carbon Binders: Mechanical, Hygrothermal, and Durability Performance, *Case Studies in Construction Materials*, *22* (2025), e04915
[8] Benmahiddine, F., *et al*., Multi-Scale Analysis of the Effects of Hysteresis on the Hydrothermal Behaviour of Biobased Materials: Application Hemp Concrete, *Construction and Building Materials*, *411* (2024), 134107
[9] Ayati, B., *et al.*, Mechanical and Hygrothermal Properties of Hemp-Silica Biocomposites, *Construction and Building Materials*, *425* (2024), 136077
[10] Aguiar, A. L., *et al*., Experimental Investigation on the Fire Performance of Wood Bioconcrete Using Cone Calorimeter, *Fire Safety Journal*, *148* (2024), 104225
[11] Wu, D., *et al*., Dynamic Hygrothermal Behavior and Energy Performance Analysis of a Novel Multilayer Building Envelope Based on PCM and Hemp Concrete, *Construction and Building Materials*, *341* (2022), 127739
[12] Charai, M., *et al*., Hygrothermal, Mechanical and Durability Assessment of Vegetable Concrete Mixes Made with Alfa Fibers for Structural and Thermal Insulating Applications, *Construction and Building Materials*, *335* (2022), 127518
[13] Bennai, F., *et al*., Assessment of Hygrothermal Performance of Hemp Concrete Compared to Conventional Building Materials at Overall Building Scale, *Construction and Building Material*s, *316* (2022), 126007
[14] El Moussi, Y., *et al*., Experimental Investigation on the Influence of Rice Straw Characteristics on the Hygric, Thermal and Mechanical Properties of Straw-Lime Concretes, *Construction and Building Materials*, *478* (2025), 141379
[15] Chennouf, N., *et al*., Hygrothermal Characterization of a New Biobased Construction Material: Concrete Reinforced with Date Palm Fibers, *Construction and Building Materials*, *192* (2018), Dec., pp. 348-356
[16] Ansari, H., *et al*., A Comprehensive Review on the Properties of Hemp Incorporated Concrete: An Approach to Low Carbon Footprint Construction, *Next Sustainability*, *5* (2025), 100075
[17] Ahmad, M. R., Chen, B., Influence of Type of Binder and Size of Plant Aggregate on the Hygrothermal Properties of Bioconcrete, *Construction and Building Materials*, *251* (2020), 118981
[18] Sawadogo, M., *et al*., Investigation of a Novel Biobased Phase Change Material Hemp Concrete for Passive Energy Storage in Buildings, *Applied Thermal Engineering*, *212* (2022), 118620
[19] Ntimugura, F., *et al*., Strength and Hygrothermal Performance of Low Carbon Insulation Materials Made of Lime Ternary Binders and Miscanthus Particles: Miscrete, *Construction and Building Materials*, *473* (2025), 141055
[20] Alioua, T., *et al*., Sensitivity Analysis of Transient Heat and Moisture Transfer in a Biobased Date Palm Concrete Wall, *Building and Environment*, *202* (2021), 108019
[21] Pietrak, K., *et al.*, Magnesium-Hemp Concrete Is Less Vapor-Permeable Than Lime-Hemp Concrete While the Cup Method Is Still Problematic, *Building and Environment*, *280* (2025), 113112
[22] Benmahiddine, F., *et al*., Experimental investigation on the Influence of Immersion/Drying Cycles on the Hygrothermal and Mechanical Properties of Hemp Concrete, *Journal of Building Engineering*, *32* (2020), 101758
[23] Lagouin, M., *et al*., Influence of Types of Binder and Plant Aggregates on Hygrothermal and Mechanical Properties of Vegetal Concretes, *Construction and Building Materials*, *222* (2019), Oct., pp. 852-871
[24] Zou, Y., *et al*., A Dynamic Hysteresis Model of Heat and Mass Transfer for Hygrothermal Biobased Materials, *Journal of Building Engineering*, *79* (2023), 107910
[25] Benmahiddine, F., *et al*., Effect of Flax Shives Content and Size on the Hygrothermal and Mechanical Properties of Flax Concrete, *Construction and Building Materials*, *262* (2020), 120077
[26] Ramirez, R., *et al*., Hygro-Thermo-Mechanical Analysis of Brick Masonry Walls Subjected to Environmental Actions, *Applied Sciences*, *13* (2023), 7, 4514

[27] Feng, C., Janssen, H., Hygric Properties of Porous Building Materials (II): Analysis of Temperature Influence, *Building and Environment*, *99* (2016), Apr., pp. 107-118
[28] Schirmer, R., Die Diffusionszahl von Wasserdampf-Luft-Gemischen und die Verdampfungsgeschwindigkeit, Ph. D. thesis, VDI-Verlag, Dusseldorf, Germany, 1938
[29] Murray, F. W., On the Computation of Saturation Vapor Pressure, *Journal of Applied Meteorology and Climatology*, *6* (1966), 1, pp. 203-204
[30] Monteith, J. L., Shatleworth, M. H., *Principles of Environmental Physics*, 4t^{h} ed., Elsevier Ltd., London, UK, 2013
[31] Gummerson, R. J., *et al*., Water Movement in Porous Building Materials – II. Hydraulic Suction and Sorptivity of Brick and Other Masonry Materials, *Building and Environmen*t, *15* (1980), 2, pp. 101-108
[32] Cammerer, W. F., *Wärme- Und Kälteschutz Im Bauwesen Und in Der Industrie*, 5th ed., Springer, Berlin/Heidelberg, Germany, 1995
[33] Castellazzi, G., *et al*., Modelling of Non-Isothermal Salt Transport and Crystallization in Historic Masonry, *Key Engineering Materials*, *624* (2014), Sept., pp. 222-229
[34] Kunzel, H. M., Simultaneous Heat and Moisture Transport in Building Components: One- and 2-D Calculation Using Simple Parameters. Ph. D. thesis, Fraunhofer Institute for Building Physics, Stuttgart, Germany, 1995
[35] Bergman, T. L., Lavine, A. S., *Fundamentals of Heat and Mass Transfer*, 8th ed., John Wiley & Sons, Hoboken, N. J., USA, 2017
[36] Alioua, T., *et al.*, Investigation on Heat And Moisture Transfer in Biobased Building Wall with Consideration of the Hysteresis Effect, *Building and Environment*, *163* (2019), 106333
[37] Seng, B., Etude expérimentale et numérique du comportement hygrothermique de blocs préfabriqués en béton de chanvre, Ph. D. thesisi, University Toulouse 3 Paul Sabatier (UT3 Paul Sabatier), Toulouse, France, 2018
[38] Ramirez, R., *et al*., Experimental Characterization of Moisture Transport in Brick Masonry with Natural Hydraulic Lime Mortar, *Building and Environment*, *205* (2021), 108256
[39] D'Altri, A. M., *et al.*, A 3-D Detailed Micro-Model for the in-Plane and Out-of-Plane Numerical Analysis of Masonry Panels, *Computers & Structures*, *206* (2018), Aug., pp. 18-30
[40] Ghiassi, B., *et al.*, Numerical study of the role of mortar joints in the bond behavior of FRP-strengthened masonry. Composites Part B: Engineering, *46* (2013), Mar., pp. 21-30
[41] Hagentoft, C. E., *et al*., Assessment Method of Numerical Prediction Models for Combined Heat, Air and Moisture Transfer in Building Components: Benchmarks for 1-D cases, *Journal of Thermal Envelope and Building Science*, *27* (2004), 4, pp. 327-352
[42] Fezzioui, N., *et al*., Numerical Study on Coupled Heat and Mass Transfer in Masonry Wall, *Proceedings*, 12th International Conference on Fluid-Flow, Heat and Mass Transfer (FFHMT 2025), Imperial College London Conference, London, UK, 2025

Paper submitted: April 22, 2025
Paper revised: June 29, 2025
Paper accepted: July 30, 2025